

Simulation of miniature optical correlator for future generation of spacecraft precision landing

Hanying Zhou, Tien-hsin Chao, Bryan Martin, and Nate Villaume

Jet Propulsion Laboratory, M/S 303-300
California Institute of Technology
4800 Oak Grove Drive, Pasadena, CA 91109-8099

ABSTRACT

Future Mars/planets explorations call for precision and even pinpoint landing. Low cost optical correlators are one of the promising enabling technologies for pinpoint landing. JPL has developed a state-of-the-art miniature optical correlator (MOC) to demonstrate its feasibility. In this paper, we describe a simulation testbed under development for measuring MOC's performance in a high-fidelity entry, descent, and landing environment, and provide our preliminary simulation result.

Keywords: optical correlator, precision landing,

1. INTRODUCTION

Future Mars/planets explorations, especially human lander missions to Mars, calls for highly accurate and precise landing of crew and equipment to successfully achieve the desired scientific objectives. To ensure maximum scientific achievement and human safety/habitability, sites acceptable for exploration will be carefully chosen in advance. During entry, descent and landing (EDL), accurate navigation will be required to guide landing crafts to the pre-selected sites. Split mission deployment (i.e., sending cargo and humans on separate lander missions) also requires precise navigation to minimize landing dispersion errors so that pre-deployed equipment and crews can be landed within close proximity. It is expected that these future missions will require stringent landing errors, e.g., within 10's meters of targeted sites.¹ This far exceeds the capability of current technology and planetary landing methodologies. The Mars Pathfinder 98 Mission design produced landing errors in excess of 150 kilometers.¹

Several new technologies are currently being explored to meet the challenge of precision landing. Among them, optical processing technology, such as automatic target recognition using optical correlator, has emerged as one of the potential enabling technologies to replace or complement the bulky Inertia Measurement Units for precision landing guiding.² An optical correlator takes advantages of shift-invariant parallel Fourier transform achieved by optical lenses at the speed of light and with minimal electrical power consumption. In operation, thousands of templates ("composite filters") are uploaded and checked against each incoming input frame in real time to detect and locate the target-of-interest in the input scene. In precision landing, landing site as well as EDL trajectory will be pre-determined by analyzing images gathered by previous imaging of the surface. This provides a great wealth of a-priori knowledge about the intended target (landing site) as well as the background and thus makes an optical correlator a perfect candidate for landing site detection and tracking. In this scenario, composite filters can be pre-synthesized prior to launch using available high-resolution maps of the pre-selected site and well designed EDL profile. Output information from the correlator is then fed back for accurate navigation control.

One of the biggest advantages of optical correlator is its high throughput for image-based target recognition/tracking processing: at least three orders of magnitude higher than a state-of-the-art digital processor could accommodate under the power/mass/volume constraints in a space environment. This is particularly attractive for landing site tracking since the spacecraft's downward velocity could be extremely high during the early stage of EDL, where the hardware implemented MOC-assisted navigation would offer a clear processing advantage over any software-based system.

The current state-of-art MOC developed at JPL features a very compact size (2"x2"x2" when fully packaged), large template format (512x512), high frame rate (1000 frames/sec for filter cycling), low power consumption (<5W), and the ability to implement near theoretical optimal filter for robust target recognition.³

Detailed technical progress in developing the MOC for spacecraft navigation applications has been described elsewhere.³ This paper focuses on the parallel work to develop a high-fidelity MOC simulator and the preliminary landing site tracking simulation of MOC in a realistic environment.

2. OVERVIEW OF THE DEVELOPMENT OF MOC SIMULATOR

In order to validate the merit of the MOC and demonstrate how the MOC can be integrated into future missions and used operationally for EDL, a rigorous quantitative assessment in a high-fidelity environment is needed. The partially TMOT-funded DSENDS (Dynamic Simulator for Entry, Descent, & Surface Landing) multi-mission EDL simulation tool at JPL, provides such a high-fidelity, mission validated, simulation environment. It is based on the mature, JPL developed Darts/Dshell multi-mission spacecraft simulator, and provides 6+ DOF flex-body dynamic capability and the ability to simulate and track multiple objects and trajectories during entry, descent, and landing on a planet or other celestial body.

We have been developing a MOC simulator in this high-fidelity environment. The goal is to perform a hardware-in-the-loop, end-to-end EDL simulation of MOC with realistic instrument imaging and GN&C interaction. To this, we will integrate the MOC into DSENDS testbed through hardware and software interfaces. The DSENDS simulator will generate trajectory information based on GN&C inputs and environmental interactions, and will then generate simulated terrain images. The images will be fed to the MOC through a VGA interface. The MOC output will be fed into the GN&C algorithm, thus closing the loop. List of mission-specific and general technical and performance metrics for measuring performance of the MOC against mission needs and performance requirements will be developed. These metrics will be incorporated into sample missions and a test suite will be generated to exercise the MOC in relation to the selected metrics. Appropriate levels of simulated performance noise will be injected (camera jitter, focus, dust, etc) as appropriate for each test sequence. Test sequences will be based on the selected metrics and performance criteria that exercise the full range of desired behaviors from the MOC and its interaction with spacecraft GN&C. Analysis of the MOC applied against a wide variety of scenarios will be performed, with representative or actual GN&C algorithms for the selected mission, a combination of actual and simulated terrain from orbit to ground, high-fidelity spacecraft dynamics (6DOF+), and sensor and actuator models for each scenario. And finally, conceptual description of how the MOC can be integrated into a GN&C environment for operational EDL use will be developed.

It is expected that this high-fidelity MOC GN&C simulator will provide superior metrics for performance prediction of MOC, and perform comparative analysis of different navigation sensors in a realistic setting.

3. PRELIMINARY DEVELOPMENT OF MOC SIMULATOR

3.1 EDL Terrain Generation Process

Since no real landscapes at the desired resolution are available for a full coverage of EDL simulation, the first step in our MOC simulator development is to generate simulated terrain image sequences. This is done by using a combination of a-priori images from available high resolution orbital imagery and simulated terrain and adding various desired visual and physical features into the landscape (i.e., rock/crater density and size, terrain slope, etc.) according to selected mission conditions and with a resolution commensurate with the ability of spacecraft instruments.

To this, we extended the DSENDS interface to the JPL Terrain server, which have the ability to use supplied Digital Elevation Models (DEMs) at a given resolution to produce higher resolution DEMs and matching graphics down to any

desired resolution with resolution-appropriate features added. In our preliminary effort, we used existing tools and techniques to generate multi-resolution terrain images centered on a MER '03 candidate landing site, Eos Chasma VM41A2. The landing site is in the floor of a valley about 40Km wide, and the landing ellipse is in the middle of the valley. The ellipse occupies <10% of the total terrain area. Because of this, during the simulation, much the other terrain is never visible for long. Therefore, we added artificial terrain only to the valley floor.

Figure 1 shows a graphical overview of the process involved in enhancing the terrain. We used a publicly available Virtual Reality Modeling Language (VRML) file of Eos Chasma to make a DEM of the landing site. The VRML file was created from Mars Global Surveyor (MGS) data. This DEM was then read into an open source graphics manipulation package, Height Field Lab, for algebraic operations on terrain. To add only features to the valley floor, we created a terrain mask which had a value near to one for the valley floor and zero elsewhere. A multiplication of this mask against artificial terrain would yield a piece of artificial terrain in the shape of the valley. Using Height Field Lab, this masked, simulated terrain was then added to the original MGS terrain. This combined terrain was then turned into the Inventor format so that the simulation visualization tool could use it.

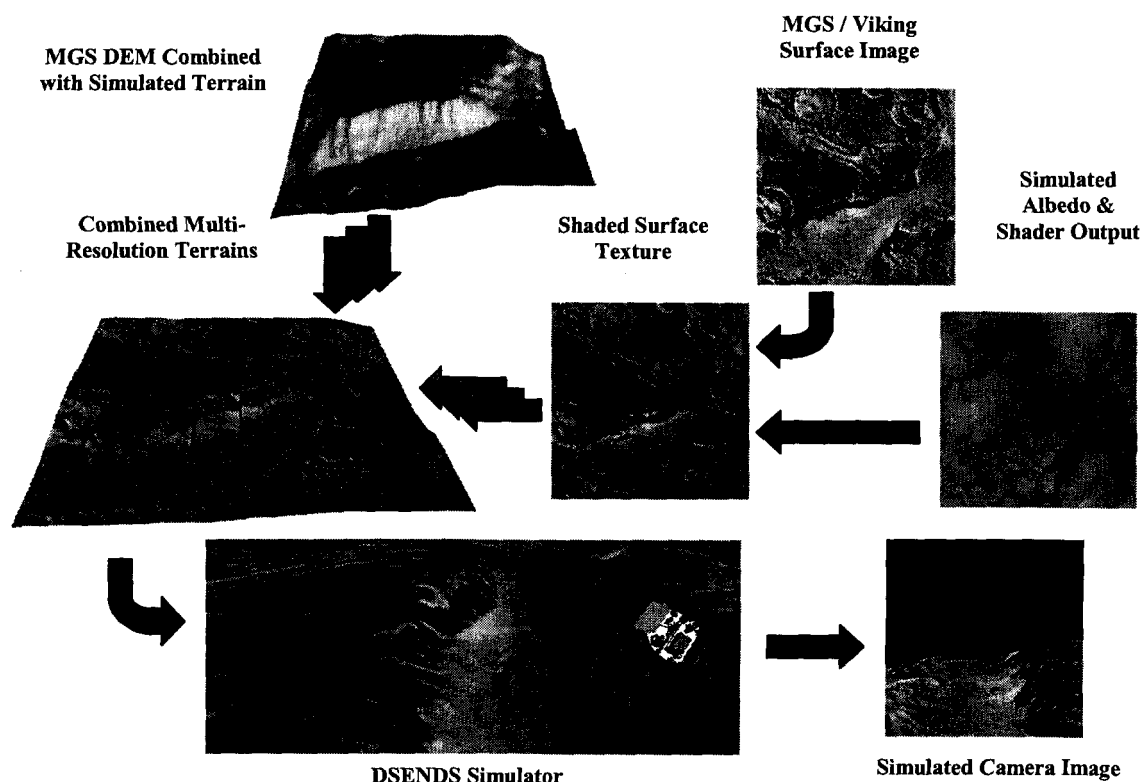


Figure 1 Terrain generation process

The simulated terrains are output in DEM format. The overall DEM geometry is rectilinear. Craters are the dominant features. The Terrain Server also produces albedo maps, which tell how much light the terrain will reflect. The albedo maps are useful for creating texture maps with Shader, an SGI visualization program that uses shadows to add authenticity to 3D objects. In the process described above, both the simulated terrain and albedo maps were masked. In this way, Shader only operated on the terrain for which we had albedo maps.

The terrain generation, masking, recombination and all translations between formats had to be done at each resolution. Because higher resolution terrains are a subset of the larger terrain, an extra clipping procedure was necessary. The original terrain and terrain mask were clipped to match the size of the simulated terrain. The clipped terrain was enhanced in Height Field Lab with fractal methods, and then combined as above with the masked simulated terrain and converted to Inventor format.

As a final step, the Shader generated texture maps were applied to each terrain. The set of inventor files were laid on top of each other, with the highest resolution (and smallest area) terrain on top, visible to the simulation camera. As a backdrop, we acquired a 30° by 45° picture of the Martian surface and mapped it onto the appropriate surface patch of a sphere with Martian radius. The features of the original VRML terrain and this planetary backdrop visually coincide.

3.2 MOC simulation model tool

The second major effort was to develop a software MOC simulation model tool and integrate it into the DSEDS spacecraft EDL simulator. It is an intermediate step toward the ultimate goal of hardware-in-the-loop, end-to-end EDL simulation of MOC. Currently the software model consists of a custom correlation filter synthesis and filter projection to SLM coding domain, correlation operator, and correlation peak-detection post processing. The simulation model tool is developed using MATLAB toolkit.

The customized correlation filter algorithm is based on OT-MACH (optimum trade-off Maximum Average Correlation Height) filter algorithm.^{4,5} The OT-MACH filter tries to balance simultaneously several conflicting performance measures such as Average Correlation Height (ACH), Average Similarity Measure (ASM), Average Correlation Energy (ACE) and Output Noise Variance (ONV), by minimizing the following energy function:

$$E(\mathbf{h}) = \alpha(ONV) + \beta(ACE) + \gamma(ASM) - \delta(ACH) \\ = \alpha \mathbf{h}^T \mathbf{C} \mathbf{h} + \beta \mathbf{h}^T \mathbf{D}_x \mathbf{h} + \gamma \mathbf{h}^T \mathbf{S}_x \mathbf{h} - \delta \left| \mathbf{h}^T \mathbf{m}_x \right|$$

The resulting optimal-tradeoff MACH filter (in frequency domain) is given by^{4,5}

$$\mathbf{h} = \frac{\mathbf{m}_x^*}{\alpha \mathbf{C} + \beta \mathbf{D}_x + \gamma \mathbf{S}_x}$$

where α , β and γ are nonnegative OT parameters. \mathbf{m}_x is the average of the training image vectors x_1, x_2, \dots, x_N . \mathbf{C} and \mathbf{D}_x are the diagonal power spectral density matrixes of additive input noise and of the training images, respectively. \mathbf{S}_x is the similarity matrix of the training images: $\mathbf{S}_x = \Sigma(X_i - M_x)^*(X_i - M_x)/N$, with M_x denoting the average of X_i .

By choosing different values of α , β and γ , one can control the OT-MACH filter's behavior to suit different application requirements. For example, when $\beta = \gamma = 0$, the resulting filter behaves much like a MVSDF filter with relative good noise tolerance but broad peaks. If $\alpha = \gamma = 0$, then the filter is more like a MACE filter, which generally gives sharp peaks and good clutter suppression but is very sensitive to distortion. For $\alpha = \beta = 0$, the filter is an ACH filter which itself is designed with high tolerance for distortion.

Unlike most ATR applications where a potential target might be embedded in an unknown and often cluttered background, here the distinguish between background and target is dependent on the target size chosen which could be constantly changing and could reach the whole frame size. It is expected, therefore, clutter/noise is not a major problem (though we still need to consider detector noise) for landing site tracking application. In contrast, the most demanding problem of filter synthesis here will be the large distortion induced by the wide range of altitude change and the spinning of the spacecraft. This means we can expect a small value of β , a high value of γ , and a somewhat in-between value of α , to emphasis the tolerance in scale, rotation, and perspective changes.

To implement the OT-MACH filter on optical correlator, one needs to find out its minimum Euclidean distance (MED) version of the filter or the SLM coding domain.⁶ To better utilize the limited dynamic range of the currently available

SLMs, we also developed a practical filter dynamic range compression technique, the histogram stretch, after using the MED projection.⁷ The procedure for this histogram stretch is rather simple. First, we calculate the standard deviation, σ , of the pixel histogram of the MED version filter. The smaller the standard deviation σ , the narrower the filter's histogram distribution. Then we find out pixels whose values are outside a certain range of pixel values, say, $\pm 3\sigma$, and assign those pixels with maximum values (in our 8-bit real-valued SLM case, it is ± 127) and linearly stretch the rest pixel values toward the maximum values.

The correlation operator simulates the MOC performance, and is capable of simulating a variety of optical implementation problems, including detector noise, SLM contrast, filter and input SLMs misalignment, etc. The correlation peak detection is based on calculation of peak-to-side-lobe ratio.

3.3 MOC Correlation Simulation

We have performed a landing site tracking simulation of MOC through the EDL sequence from orbit to ground. Our preliminary effort has focused on the simulation with a fast downward spacecraft during early stage of EDL and its multiple target tracking ability.

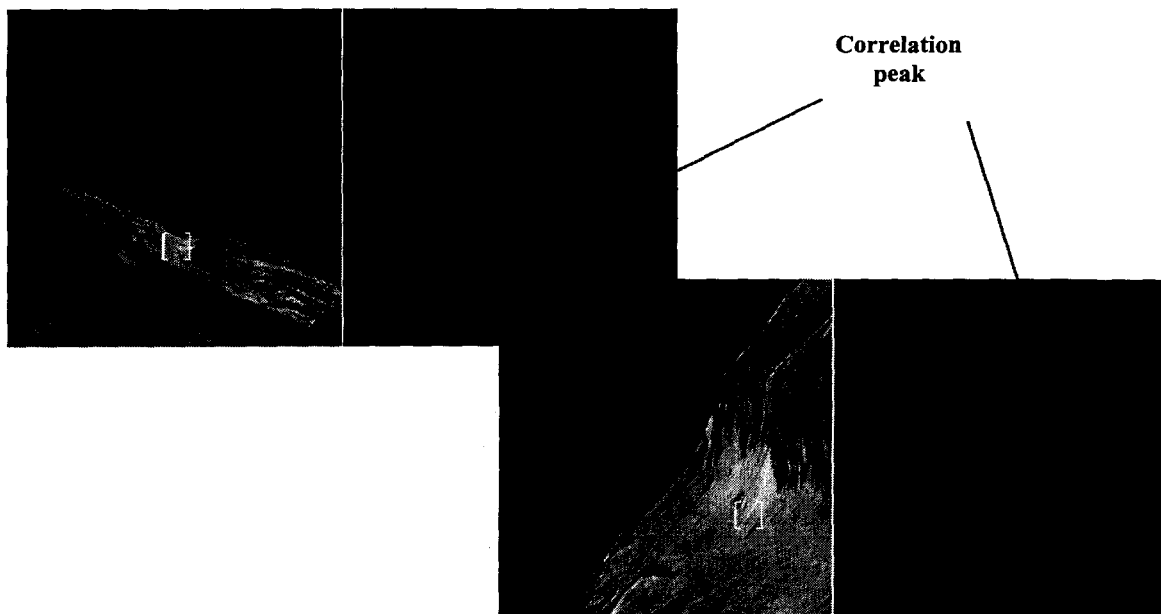


Fig.2 Landing site tracking with a fast downward and full rotation spacecraft

As depicted in Figure 2, the landing site (a MER '03 candidate site, Eos Chasma VM41A2) is in the floor of a valley. The simulation scene starts at about 55km. The spacecraft quickly approaches the pre-selected landing site with a downward speed about 7km/s and with fast spinning. At this high speed of spinning and downward, no known software-based system is potentially able to meet the throughput demand of image processing. Only the hardware implemented MOC-assisted navigation could offer the necessary processing throughput it needs. In our simulation we used only 8 filters to accommodate the wide range of altitude changes and full rotations of the spacecraft, and demonstrated correlator's ability to lock on to the landing target through the EDL sequence.

Due to the wide range of altitude change, it is unrealistic to track a single target from orbit to the ground in precision landing. In fact, as the lander descends, the original target will get larger and larger, and at the same time more and more fine features of the targeted surface appear. At some point the correlator will have trouble discerning the originally defined landing target when the increased target size is close or beyond correlator's field of view and/or when increased

fine new feature are now in view. Concerns over potential wind effect during parachute phase as well as the fact that the spacecraft is fast spiraling also promotes the need for multiple target tracking ability to ensure the proper tracking. To these reasons, we simulated the multiple-target tracking ability of MOC as altitude and pointing direction change. As seen in Figure 3, after tracking a first target and before it nears the edge of the frame (spiraling out, for example, since the spacecraft is rotating), the MOC picked up a new target from the frame. By having both target active for a short while we provide a smooth transition from the first target to the second target rather than switching suddenly.

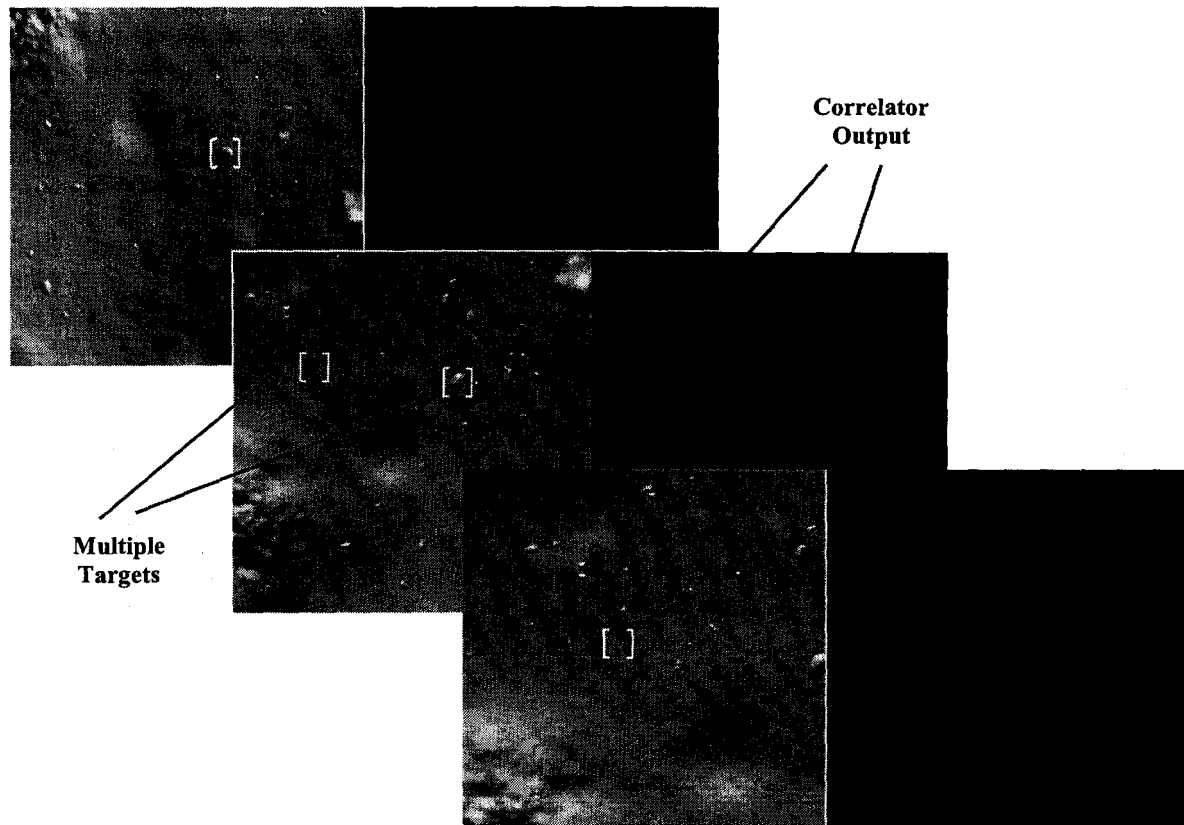


Figure 3. Multiple target tracking ability

3.4 MOC accuracy

The MOC accuracy is determined largely by two factors: terrain height (or pixel resolution of the terrain) and correlation peak localization.

The pixel resolution of the terrain p can be found by the simple geometric relationship: $p = 2h \tan(f/2)/N$, where h is the height above the terrain, f is the field of view of the camera, and N is the pixel number in one dimension of the correlator. An example is worked out in Table 1 for $f=30^\circ$ and a 512×512 correlation frame size.

Table 1 Pixel resolution of terrain

Terrain height h	100km	50km	10km	1km
Resolution p (m/pixel)	104	50	10	1

In practice since camera is almost always looking at the terrain from an angle (especially during the early stage of EDL), this means the terrain in the foreground may be closer than the terrain in the rest part of the image, and hence the resolution is also slightly different across the image.

The second factor, the correlation peak localization, depends on the quality of the correlation peak itself as well as the accuracy in target center selection (during filter synthesis). From our experience in simulation and optical implementation, we have found both can be easily controlled within few pixels range (1~3 pixels). This means that the ultimate accuracy of MOC would be well within few meters when terrain height is about 1km and less thereafter. This far exceed the requirement of the precision and pinpoint landing dispersion.

4. CONCLUSION

We have described our recent effort on the development of a software model MOC simulator for spacecraft navigation application. The main effort was focused on the generation of terrain image sequence and the development of correlator operation model of MOC. A preliminary MOC simulation through the EDL sequence from orbit to ground is performed to demonstrate the feasibility of MOC for precision landing site tracking.

Further development in the simulator is underway, with the ultimate goal to include interactive software and hardware (hardware-in-the-loop) tests on the DSENDS simulator to facilitate simulation testing.

ACKNOWLEDGMENTS

The research described in this paper was carried out by the Jet Propulsion Laboratory, California Institute of Technology, under a contract with the National Aeronautics and Space Administration and was funded partially by the Telecommunication and Mission Operation Technology (TMOT) program at JPL.

REFERENCES

1. A. Benjamin, G. Smit, J. A. Cuseo, and S. D. Lindell, "Overview: precision landing/hazard avoidance concepts and MEMS technology insertion for human Mars lander missions," Proceedings of AIAA/IEEE Digital Avionics System Conference, V2, pp. 8.5-18-8.5-25, 1997.
2. Tien-Hsin Chao, Hanying Zhou, and George Reyes, "Spacecraft Navigation Using Optical Correlator", SPIE v.4734, p108-112, 2002
3. Tien-Hsin Chao, Hanying Zhou, and George Reyes, "Compact 512x512 Grayscale Optical Correlator", SPIE v.4734, p9-12, 2002
4. B. V. K. Vijaya Kumar, D. Carlson, and A. Mahalanobis, "Optimal trade-off synthetic discriminant function filters for arbitrary devices," *Opt. Lett.* 19, pp. 1556-1558, 1994.
5. V. Laude and Ph. Refregier, "Multicriteria characterization of coding domains with optimal Fourier spatial light modulator filters," *Appl. Opt.* 33, pp. 4465-4471, 1994.
6. R. D. Juday, "Optimal realizable filters and the minimum Euclidean distance principle," *Appl. Opt.* 32, pp. 5100-5111, 1993.
7. Hanying Zhou, Tien-Hsin Chao, and George Reyes, "Practical saturated filter for grayscale optical correlator using bipolar-amplitude SLM," SPIE 4043, 2000.